DEPARTMENT OF THEORETICAL PHYSICS
UNIVERSITY OF LUND
SÖLVEGATAN 14 A
S-223 62 LUND SWEDEN

LU TP 80-6
September 1980

ON HIGH ENERGY LEPTOPRODUCTION

Bo Andersson, Gösta Gustafson, Gunnar Ingelman, Torbjörn Sjöstrand

Department of Theoretical Physics
University of Lund
LUND, Sweden

Abstract: The particle distributions and the event structures in high energy leptoproduction are considered in a model where perturbative QCD is used to compute the cross sections to order α_s and the Lund jet model is used for the soft hadronization process. The model is found to be in agreement with data from the European Muon Collaboration. We indicate how a one-particle trigger can be used to study an enriched sample of two forward jet events, and exhibit a useful experimental test for the existence of such events with the properties predicted by perturbative QCD. We also indicate how to gain further information on the confinement and soft fragmentation mechanisms.

LU TP 80-6
September 1980

On High Energy Leptoproduction

Bo Andersson, Gösta Gustafson, Gunnar Ingelman, Torbjörn Sjöstrand

Department of Theoretical Physics
University of Lund
LUND, Sweden

Abstract: The particle distributions and the event structures in high energy leptoproduction are considered in a model where perturbative QCD is used to compute the cross sections to order α_s and the Lund jet model is used for the soft hadronization process. The model is found to be in agreement with data from the European Muon Collaboration. We indicate how a one-particle trigger can be used to study an enriched sample of two forward jet events, and exhibit a useful experimental test for the existence of such events with the properties predicted by perturbative QCD. We also indicate how to gain further information on the confinement and soft fragmentation mechanisms.

Introduction

In this paper we will study leptoproduction on proton targets at high energies. Our basic assumption is that there are two space-time scales involved. On the short scale, characterised by the QCD parameter $1/\Lambda \sim 0.4$ fm , the coloured objects behave like essentially free particles and perturbative QCD is applicable. In particular a quark can emit hard gluon bremsstrahlung at a rate determined by the strong effective coupling constant $\alpha_s(Q^2)$. The long scale corresponds to the soft hadronization where the coloured objects are connected by colour force fields. In order to compare the predictions from perturbative QCD (as e.g. the transverse momentum increase with energy) to the experimental data it is necessary to take the soft hadronization into account in a consistent way. The aim of this paper is twofold, firstly to check the predictions from perturbative QCD, and secondly to gain information about the soft hadronization.

Except for the "ordinary" single quark (antiquark) jets (which we will subsequently call q-jet events) there are two dynamically different 2-jet event situations to lowest order in α_s . In the first one the quark (or antiquark) radiates off a gluon (cf fig. 1a) (we will call these (qg) events) and in the second one a gluon is split into a quark-antiquark pair ($(q\bar{q})$-events) (cf fig. 1b). The cross sections for these different processes are given e.g. in ref. [1].

For the soft hadronization we will use the model for quark and gluon jets, described in refs. [2-6]. It presents a relativistically invariant and causal way of partitioning the energy and momentum of a colour force field among the final state mesons. The dynamics of the force field is that of the massless relativistic string, stretched between a quark and an antiquark. The relativistic invariance of the model implies e.g. that we avoid the selection of a fixed space-point in a particular Lorentz frame (e.g. the cms) to connect the jets.

A useful property of the model is the fact that the production process basically is of a stochastic nature and that the model therefore is easily implemented in terms of a Monte Carlo generation process [5,6].

We note that the differential cross sections from perturbative QCD contain divergencies which physically correspond to the emission of soft or collinear gluons. In our model there is a natural cut off and a smooth transition between the q-jet and 2 -jet events respectively [6,7].

Most of the considerations in this paper are connected to the fragmentation properties of the forward moving objects, i.e. to the event structure outside the target fragmentation region. We have in ref. [8] presented a model for baryon fragmentation and we will in forthcoming publications come back to the baryon fragmentation region in leptoproduction events.

The model is described in section 2 and our results are presented in section 3. We end with some comments in section 4.

2. The model

A. The perturbative part

There are to lowest order in α_s from perturbative QCD two kinds of corrections to the parton model results. They correspond to the Feynman graphs of figs. (1a,b) . There is to the same order in α_s the vertex correction in fig. (1c) to take into account for the relative probability to obtain q-jet, (qg)-jet and $(q\bar{q})$-jet events. The corresponding analytical expressions for the cross sections are given in e.g. ref. [1] .

To evaluate the cross sections it is necessary to make use of the structure functions for the proton constituents. We will in general use a Q^2-independent structure function $F_2(x)$ as obtained from SLAC data [9] . In order to describe high energy muon data from FNAL and CERN [10] this function was modified for $x < .2$ so that F_2 instead of decreasing for small x is increasing to .5 at $x=0$. For the gluons we use the distribution

$$x\,G(x) = \tfrac{1}{2}(1+\eta)(1-x)^{\eta} \qquad (1)$$

with $\eta = 5$. We have also investigated the sensitivity to the choice of the structure functions and studied e.g. the Q^2-dependent parametrization by Glück and Reya [11] and by Buras and Gaemers [12] . Generally the results presented here do not depend on this choice unless the softness of the gluon distribution is changed drastically, e.g. $\eta \gtrsim 12$ as in ref. [12].

In the process in fig. 1a the quark (or antiquark) radiates off a gluon (a (qg)-event). These events give the dominating contribution to 2 jet events for the larger values of x_B and it is interesting to note that the gluon emission probability is essentially only dependent on the total hadronic cms energy W for $x_B > .15$. However, since the x_B distribution is peaked at small values one must also take the x_B dependence into account when comparing with data.

We return to the treatment of the divergencies in the expressions corresponding to soft or collinear gluon emission below. In the process in fig. 1b a gluon is split into a quark-antiquark pair. These $(q\bar{q})$-jet events then correspond to a quark and an antiquark jet emerging from a colour octet target remnant. Usually the energy is very unevenly shared between the two jets, one being very soft. The relative cross section for these $q\bar{q}$-jet events is a complicated function of W and Q^2 (or W and x_B) and it dominates over the qg-jet events for small values of x_B ($x_B \lesssim .08$ when $W \lesssim 20$ GeV).

B. The soft hadronization

The Lund soft hadronization jet model is described in detail in refs. [2,3,4] and in its Monte Carlo generation version for e^+e^- annihilation events in ref.[5,6]. We will therefore in this paper only comment upon a few particular features which are of interest for the application to leptoproduction events.

The model is relativistically invariant and causal and based on a semiclassical treatment of the dynamics of the massless relativistic string.

If a quark and an antiquark go out from one space-time point with large momenta in opposite directions, a linear colour force field (or colour flux tube) is stretched between them. This field breaks into small pieces (mesons) by the production of

quark-antiquark pairs, which are pulled apart by the field.

One basic assumption in the model (resulting in e.g. polarization properties for inclusively produced Λ^0-particles [13]) is that the force field has no excited transverse degrees of freedom during the soft hadronization. Therefore transverse momentum is locally conserved at each breaking point. Thus the quark and the antiquark of a produced pair have equally large and opposite transverse momenta $p_\perp$. In such a force field large transverse masses are suppressed and we obtain in ref. [4] a Gaussian distribution in $p_\perp$ together with a suppression of the heavier strange quarks. We will here use $\langle p_\perp^2 \rangle = (.44\ \mathrm{GeV/c})^2$ [19].

Because the produced quark-antiquark pairs have compensating flavours there is a strict ordering of the mesons with regard to flavour (called rank), which on the average also agrees with the ordering in rapidity. However, we note that the ordering with regard to production times is Lorentz frame dependent. Those mesons which are slow in one Lorentz frame are also the ones produced first in that frame. In this sense it is an "inside-out cascade". Thus with a large boost along the leading quark we obtain a Lorentz frame in which the first rank meson is also produced first in time. The assumption that the probability for a particular break up situation is determined by the available number of final states then implies an iterative structure similar to that in cascade jet models [14] , which is easily implemented in a Monte Carlo generation procedure.

A relativistically invariant generalization of a one-dimensional linear force field to three dimensions is provided by the dynamics of the massless relativistic string [3,15]. On such a string it is possible to have a localized excitation, a kink, which carries energy and momentum and moves with the velocity of light. This kink is pulled back by the string with twice the force acting on an endpoint quark. Thus it behaves like a gluon (in QCD with N colours the ratio between the forces on a gluon and a quark is expected to be $2/(1-1/N^2)$, i.e. 2 for infinitely many colours). In refs.[2,6,7] we have used such a kink as a model for a gluon and calculated the gluon jet fragmentation with the same methods as we used for the quark jets.

The idea is thus that in the initial perturbative period, in e.g. an e^+e^--annihilation event, gluon emission corresponds in our model to a kinklike excitation on the force field. In the following soft hadronization the forcefield is stretched in a smooth way, without any further transverse excitations, and breaks into pieces, hadrons, by the production of quark-antiquark pairs as described above.

The stretching and breaking of the stringlike field in an $e^+e^- \to q\bar{q}g$ event is illustrated in fig. 2 (cf refs. [6,7])
A very essential feature of the model is that the force field is stretched from the quark to the antiquark <u>via</u> the gluon. This implies that the mesons are produced around two hyperbolae in momentum space as indicated in fig. 3a. An asymmetry of the type predicted in ref. [7] is actually observed by the JADE-collaboration at PETRA [16].

The model also provides a natural cut off for the divergencies connected to soft and collinear gluons. For a collinear gluon the energy in the field between the gluon and the quark (or antiquark) is so small that it cannot break and produce a meson at the end. The first break will then be on the other side of the kink and the leading (first rank) meson will contain the whole string piece between the quark and the kink. The gluon and the quark will then look just like a single quark jet. We find also a smooth transition between the 3-jet and 2-jet events in e^+e^--annihilation. For a rather small angle between the gluon and the quark, the distribution of mesons in momentum space will be as indicated by the shaded area in fig. 3b.

In the case of a soft gluon we also obtain an effective 2-jet event if the energy of the gluon is so small that it stops before the string breaks the first time. The effect of the gluon will then only be a small $p_\perp$ broadening of the jet, cf. fig. 3c.

The actual cut offs used in the present calculations are those given in ref. [6]

$$M_{qg},\ M_{\bar{q}g} \gtrsim 3\ \mathrm{GeV}$$
$$\frac{M_{qg}\cdot M_{\bar{q}g}}{M_{q\bar{q}}} \gtrsim 2\ \mathrm{GeV} \qquad (2)$$

where M_{qg} is the invariant mass of the quark and the gluon etc.

When applying the same method to a leptoproduction event we note that in case of (qg) jets, if the photon hits a quark the target remnant is a colour antitriplet. Apart from the particles in the target fragmentation region we expect the same result as if it were an actual antiquark (cf ref. [3]). In case of $(q\bar{q})$ jets the outgoing quark and antiquark jets are both connected to the target remnant which is now in a colour octet state, just like a gluon. Again, if we are not studying the target fragmentation region we can use the same calculations with the gluon taking the place of the target remnant.

C. Primordial $k_\perp$

For a study of the transverse momenta of the final state hadrons it is necessary to take into account the "primordial" $\bar{k}_\perp$ of the quark or gluon struck by the virtual photon. Based on the considerations in ref.[3] we treat this by letting the jet axis "swing" around the direction of the momentum transfer $\bar{Q}$ with a Gaussian $\bar{k}_\perp$ distribution. We would from ref. [3] have expected that $k_\perp$ is at most half the proton mass, but we will in the following consider different values for the Gaussian width. This means that the final state particles will obtain a fraction of the primordial $\bar{k}_\perp$ which is roughly proportional to z . It has been suggested that this correlation between z and $k_\perp$ could be used to determine $\langle k_\perp^2 \rangle$ from the relation

$$\langle p_\perp^2 \rangle(z) = \langle p_\perp^2 \rangle_0 + z^2 \langle k_\perp^2 \rangle \qquad (3)$$

However, Monte Carlo studies indicate that this will be very difficult. Such an effect is drowned in the broadening of the 2-jet events, **because also the contributions to $p_\perp$ from the soft hadronization and perturbative QCD depend on z**, see fig.8.

Another way, which also turns out to be unsuitable according to our results, would be to determine the thrust axis for each event and compare this axis with the $\bar{Q}$-direction. Even if the momenta of both neutral and charged particles are measured accurately we find that the signal to noise ratio is too small for a determination of $k_\perp$.

3. Results

All results presented here correspond to a muon energy of 280 GeV and with cuts similar to those used by the European muon collaboration [17], namely: $20 < \nu < 260$ GeV , $W^2 > 40$ GeV^2 and $Q^2 > 5$ GeV^2 .

A. The gross features of the event structures

In order to get a general feeling of the event structures emerging from the q-jets, (qg)-jets and $(q\bar{q})$-jets respectively we present in fig. 4a,b,c the superimposed one particle densities for 2000 events of each kind in a (z,p_x) plot.

The light cone variable z which is the natural theoretical variable used in refs.[2,3,4] and in section 2 is very close to the experimentally more easily determined variable $z_\ell = \frac{p_\ell}{\nu}$. The subscripts ℓ and $\perp$ stand for the longitudinal and transverse directions with respect to the momentum transfer $\vec{Q}$ and for 2-jet events x corresponds to the transverse direction in the 2-jet event plane. We have used the cutoffs defined in eq.(2) above to distinguish between the different event situations. The actual percentage of the different types of events as a function of W is shown in fig. 4d,e for two different x-values.

The general features are evidently that

1. Both the (qg)-jet and ($q\bar{q}$)-jet events are much broader in transverse directions than the q-jet events. The mean transverse momentum for large z-values ($z > .1$) is .71 GeV/c for the (qg)-jet events, 0.51 GeV/c for the ($q\bar{q}$)-jet events and 0.37 GeV/c for q-jet events.
2. There are also fewer fast particles in the 2-jet events. In fig. 5 we present the single particle inclusive z-spectra for 1- and 2-jet events respectively. However this difference is hard to observe directly. If we e.g. enhance the number of 2-jet events by demanding a particle with large $p_\perp$ we also obtain a biased sample with regard to the z-spectrum.
3. There is a very unequal partitioning of energy among the two jets for 2-jet events. In fig. 4 the events are organized in such a way that the quark jet in qg-jet events is on the upper side ($p_x > 0$) while for ($q\bar{q}$)- jet events $p_x > 0$ corresponds to the "harder" jet in all cases (there is evidently no difference between the quark or antiquark jet in general). For a muon beam energy of 280 GeV the energy partition is on the mean in the ratio 0.57 for the gluon to quark jet for qg-jet events while it is 0.16 for the "weak" to "hard" jet in $q\bar{q}$-jet events.

For the actual mixture of the three event classes we obtain the $p_\perp$ distributions shown in figs. 6,7,8 together with preliminary data from the European muon collaboration [17] .
We have used values of $\langle k_\perp^2 \rangle = 0.36\ (\mathrm{GeV}/c)^2$, broken line, and $0.64\ (\mathrm{GeV}/c)^2$, full line. It is evident that the higher $k_\perp$-value is needed to obtain good agreement with the data. We note however, that for the highest z-bin ($0.4 < z < 1$) our model gives somewhat low values for $\langle p_\perp^2 \rangle$ in the low W-region, as compared to the EMC data but not compared to BEBC data [20].

As mentioned above and from the discussion in ref. [3], we would expect a rather small primordial $k_\perp$ coming from the motion of the quarks within the incoming proton. This $k_\perp$ would be balanced in the target fragmentation region. We think that the large $k_\perp$ needed to fit the data is an indication of soft gluon radiation as treated e.g. in ref. [21]. If this is the case, then this part of the $k_\perp$ will be balanced in the central plateau insted of in the target fragmentation region. However, as long as we study mainly particles in the current fragmentation region we think that the effect of the soft gluons can be simulated by an increased primordial $k_\perp$. We want to return to this point in a later publication.

In fig. 9 we show the z spectrum for charged particles. Besides a comparison between EMC data and the model presented in [4,6], we also indicate the further softening of the spectrum obtained when the effects of soft gluon emission are included. These effects, which do not significantly alter the transverse momentum properties of the jets, will be further studied in a forthcoming paper [19].

B. Tests of the pertubative part

Even if the predicted increase in $p_\perp$ seems to agree well with the experimental data, the basic prediction of perturbative QCD, namely the presence of 2-jet events rather than a single forward jet, which grows fatter with increasing energy, should be tested more thoroughly. The 2-jet particle structure defines a plane such that the transverse momentum distributions in the plane and out of the plane are different. As this feature already has been observed in e^+e^--annihilation [18] it would be a demonstration of a very strong dynamical difference, and a break down of the simple quark parton model interpretation, if it is not found also in leptoproduction.

A simple way to get an enriched sample of 2-jet events is to use a single particle $p_\perp$-trigger. In case we trigger on a particle with $z > 0.1$ and with $|\bar{p}_\perp| > 1.25$ GeV/c the number of 2-jet events will be enhanced to ≃ 70% instead of 22% without any trigger. By increasing the required value in $p_\perp$ an even cleaner sample will be obtained, e.g. $|\bar{p}_\perp| > 1.5$ GeV/c gives 83% 2-jet events, but of course this also reduces the statistics.

In fig. 10 we show (full line) the charged particle distributions in our model in $p^2_{\perp in}$ and $p^2_{\perp out}$ with respect to a plane defined by $\tilde{Q}$ and $\bar{p}_{\perp,trigger}$ if we use a single particle trigger with $z > 0.1$ and $|\bar{p}_{\perp,tr}| > 1.25$ GeV/c . We also show (dashed lines) the results for a "fat" 1-jet model in which the $p_\perp$-width is increased to give the same trigger rate as for our model.

We note, however, that even if such a planar property is observed it is not evident that this is due to a 2-jet structure. A simple way to demonstrate the occurrence of two jets in the experimental data is to study how the transverse momentum is compensated. To that end we again use a single particle trigger with large transverse momentum $\bar{p}_\perp = \bar{p}_{\perp,tr}$ with respect to the $\tilde{Q}$-axis. Then define two directions $\bar{e}_1$ and $\bar{e}_2$ in the plane through $\tilde{Q}$ and $\bar{p}_{\perp,tr}$ in accordance with fig. 11 . For each observed particle with $z > .1$ define the two momentum components $p_{\perp 1}$ and $p_{\perp 2}$ in the plane as indicated in fig. 11 , counted positive in the trigger side direction. Thus we always have $p_{\perp 1} < p_{\perp 2}$. Superimposing data from many events we obtain in our model calculations a clustering around both directions $\bar{e}_1$ and $\bar{e}_2$ as shown in fig. 12 a . This result is due to the fact that in general there are several particles in each jet. We note that the region of large negative $p_{\perp 1}$ and $p_{\perp 2}$ values is populated by particles belonging to the gluon jet. For a model with "fat" single jets instead of 2-jets we find, as shown in fig. 12b , only a broad band, along the direction $\bar{e}_2$, caused by total transverse momentum conservation. In this way the mean value of $p_{\perp 2}$ will vary with $p_{\perp 1}$ in different ways for the two models as can be clearly seen in fig. 12c.

C. Test of the soft hadronization. The nature of gluon fragmentation.

In section 2 and in ref. [7] we have shown that our gluon jet model, in which the colour force field is stretched between the colour triplet and antitriplet via the gluon, implies non-trivial multiplicity and angular asymmetries. An analysis like the one given in ref. [7] for e^+e^--annihilation works even better for leptoproduction because the jet axis of the target fragmentation jet (in the hadronic cms) is known from the start.

We have found that the same asymmetry should be possible to study directly in the laboratory frame from an investigation of the low z region ($z \lesssim 0.05$ at SPS energies). In our model, for z-values below ~ .05, which corresponds to the hadronic cm, the force field for $(q\bar{g})$ events bends towards the gluon side.

The particles then found on the quark side are the result of the nonperturbative broadening of the gluon side jet. Hence, using a positive particle with $z > 0.1$, $p_\perp > 1.25$ GeV/c to define the quark jet side of a 2-jet event, we expect the $z \cdot D(z)$ fragmentation function for charged particles to be considerably lower on the quark side (fig.13a). However, since part of this effect might be expected simply from the assumption of a softer gluon than quark jet, an even more revealing distribution is $\langle p_{\perp in} \rangle (z)$. This will rise approximately linearly with z on the gluon side while on the quark side it will be roughly constant up to the hadronic cm and then start rising (fig. 13b). As alternative schemes for the soft hadronization process for 2-jet events one could imagine e.g. two independent jets emerging in the laboratory frame or three independent jets emerging from the origin in the cms (one corresponding to the target fragmentation).

In the former case there will be a rise on both sides all the way, while in the latter case both sides will show essentially flat spectra for low z . To be able to discriminate between the different possibilities above, one should have at least a hundred good triggers.

4. Concluding remarks.

We have presented a combined application of lowest order perturbative QCD and the Lund soft hadronization model for the description of high energy leptoproduction. This model seems to be in agreement with the preliminary results from the European Muon Collaboration, although we note a difference in the mean squared transverse momentum $\langle p_\perp^2 \rangle$ for the region of small W^2 and large z .

We have in this model found that a useful trigger situation in order to enhance the 2-jet events very considerably is a single particle trigger with $z > 0.1$ and $|\bar{p}_\perp| > 1.25$ GeV/c . We indicate a method to check the two-jet nature of the events and also predict some particular asymmetries for small z-values which are connected to the gluon properties in our model.

We have found that there are in general only small flavour correlations to be expected and that it is very difficult to disentangle the properties of the so-called primordial $k_\perp$-distribution. The large primordial $k_\perp$ needed is, we believe, an indication for soft gluon radiation [21]. If so, this $k_\perp$ should be balanced in the central plateau rather than in the target fragmentation region. We want to study this effect further in a later publication.

The natural extension of this investigation to the properties of the target fragmentation region and to the investigation of charm production will be presented elsewhere.

References

1. G. Altarelli, G. Martinelli
   Phys. Lett 76B (1978) 89
2. B. Andersson, G. Gustafson, C. Petersson
   Zschr. f. Physik C1 (1979) 105
3. B. Andersson, G. Gustafson
   Zschr. f. Physik C3 (1980) 22
4. B. Andersson, G. Gustafson, T. Sjöstrand
   LU TP 80-1 (to be published in Zschr. f. Physik C)
5. T. Sjöstrand, B. Söderberg
   LU TP 78-18
6. T. Sjöstrand
   LU TP 80-3
7. B. Andersson, G. Gustafson, T. Sjöstrand
   Phys. Lett. 94B (1980) 211
8. B. Andersson, G. Gustafson, I. Holgersson, O. Månsson
   LU TP 80-5
9. We have used the parametrization of SLAC-data presented in ref. [1]
10. B.A. Gordon et al.
    Phys Rev. Lett. 41 (1978) 615

    EMC-collaboration, preprint CERN-EP/79-158
11. M. Glück, E. Reya
    Nucl. Phys. B130 (1977) 76
12. A.J. Buras, K.J.F. Gaemers
    Nucl. Phys. B132 (1978) 249
13. B. Andersson, G. Gustafson, G. Ingelman
    Phys. Lett. 85B (1979) 417
14. A. Krzywicki, B. Petersson
    Phys. Rev. D6 (1972) 924

    F. Niedermayer
    Nucl. Phys. B79 (1974) 355

    B. Andersson, G. Gustafson, C. Peterson
    Nucl. Phys. B135 (1978) 273

    R.P. Feynman, R.D. Field
    Nucl. Phys. B136 (1978) 1
15. X. Artru
    Orsay preprint LPTHE 78/25
16. A. Petersen
    Results from JADE on QCD in e^+e^- annihilation; contribution to "XVth Rencontre de Moriond", March 1980
17. EMC-collaboration, preprint CERN-EP/80-119, CERN-EP/80-130
18. P. Söding
    Rapporteur talk at the EPS International Conference on High Energy Interactions, Geneva 1979

19. B. Andersson, G. Gustafson; in preparation.
20. ABCDLOS-collaboration, preprint CERN-EP/80-66
21. G. Parisi, R. Petronzio
    Nucl. Phys. B154 (1979) 427

    R. Baier, K. Fey
    Bielefeld preprint BI-TP 80/10

Figure captions

Fig. 1 Feynman diagrams giving the corrections to order α_s to the pointlike quark-current cross sections. The current is denoted by a wavy line, the gluon by a spiralling line and the quarks by a continuos line.

Fig. 2 The space-time development of a quark-antiquark-gluon event. The quark and antiquark move along the directions marked q and $\bar{q}$ and are at the endpoints of a string field. The gluon is a pointlike energy-momentum carrying piece of the string moving along the direction g, thereby causing a triangular shape of the outmoving string field. The field breaks by the production of $q\bar{q}$-pairs and the directions of the final state mesons are marked by arrows when they become independent entities. (Note that the slowest mesons in the cms are the first ones to emerge, and also take the largest pieces of the string.)

Fig. 3 The momentum space distribution of the final state particles which appear in the mean along two hyperbolae. The size of the hatches indicates the size of the transverse momentum fluctuations in a string field without excited transverse degrees of freedom.

a) is for a general case while b) illustrates the case of almost collinear gluon and quark momenta and c) the case of a soft gluon.

Fig. 4 Density plot for charged particles, projected on the (z,p_x) plane, where $z = \frac{p_\ell}{\nu}$ with ℓ along $\vec{Q}$ and x transverse to $\vec{Q}$.

a) q-jet events

b) qg-jet events, $p_x > 0$ corresponds to the quark side in the event plane.

c) $q\bar{q}$-events, $p_x > 0$ corresponds to the "harder" jet in the event plane.

Percentage of qg events (full line) and $q\bar{q}$ events (dashed line) as a function of W for x = 0.05 (d) and x = 0.1 (e)

Fig. 5 The charged particle inclusive z-distribution. The full line is for 1-jet events while the broken line corresponds to 2-jet events.

Fig. 6 The transverse momentum distribution of all charged particles for different z- and W^2-bins.

a) $.2 < z < .4$ $\quad 40 < W^2 < 160$ GeV^2

b) $.4 < z < 1.$ $\quad 40 < W^2 < 160$ GeV^2

c) $.4 < z < 1.$ $\quad 280 < W^2 < 400$ GeV^2

Fig. 7 The mean squared transverse momentum for different z-bins ($0.1 < z < 0.2$, $0.2 < z < 0.4$, $0.4 < z < 1$) is shown as a function of the squared cm hadron energy W^2 together with data from EMC [17] and ABCDLOS [20].

Fig. 8 The mean squared transverse momentum as a function of z^2. The curves show the contribution from:

I: the fragmentation process as described by our cascade model

II: 1st order QCD processes

III: primordial $k_\perp$, $\langle k_\perp^2 \rangle = 0.64$ (GeV/c)^2

IV: our model when all contributions are included. It should be noted that the $p_\perp$ broadening coming from the decay of instable particles is included in each of the curves, and hence there is some double counting between I, II and III. In fact, the $p_\perp$ broadening coming from decays is a minor effect, but decays must be included to give the correct z spectrum.

Fig. 9 Distributions in z for charged particles. EMC data are compared with the "standard" Lund model, dashed, and with the model including effects from soft gluon emission, full line.

Fig. 10 The charged particle transverse momentum distribution in (a) and out (b) of the event plane defined by $\vec{Q}$ and $\vec{p}_{\perp,tr}$ for a single particle trigger with $z > 0.1$ and $|\vec{p}_{\perp,tr}| > 1.25$ GeV/c . The full curve corresponds to the model described in this paper while the dashed curve corresponds to a "fat" 1 jet model with $p_\perp$-width of 0.60 GeV/c. The cuts $W^2 > 200$ GeV^2 and $x > .05$ have been made to isolate the region where the rate of qg-events is larger.

Fig. 11 The geometry used to study how $p_\perp$ is compensated. Full line on left side is the trigger particle, the dash-dotted line gives the momentum sum of the remaining particles. For a particle (indicated with full line on right side) we may define $p_{\perp 1}$ and $p_{\perp 2}$ along the dashed line, counted positive in the trigger side direction, hence $p_{\perp 1} < p_{\perp 2}$. (Only the components in the plane are used.)

Fig. 12 Density plots ($p_{\perp 2}$,$p_{\perp 1}$) for the fastest charged particle (possibly excepting the trigger) in events with $p_{\perp,tr} > 1.25$ GeV/c and $z_{tr} > 0.1$. In fig. 12a are the results obtained from our 2-jet model, while 12b is a 1-jet model in which the σ of the primary meson $p_\perp$ distribution was raised from 0.44 to 0.60 GeV/c, to give the same trigger rate as in the 2-jet model. The cuts $W^2 > 200$ GeV^2 and $x > .05$ have been made to isolate the region where the rate of qg-events is larger.

The variation of $\langle p_{\perp 2} \rangle$ as a function of $p_{\perp 1}$ is plotted in 12c for the 2-jet model (full line) and the "fat" 1-jet model (dashed line).

Fig. 13 a) Fragmentation function for charged particles in the low z region on the trigger side, dashed, and on the opposite side, full line, according to our 2-jet model using a positive trigger with $p_{\perp,tr} > 1.25$ GeV and $z_{tr} > 0.1$.

b) Average transverse momentum in the plane defined by the trigger and the $\vec{Q}$ directions, with curves as in a).

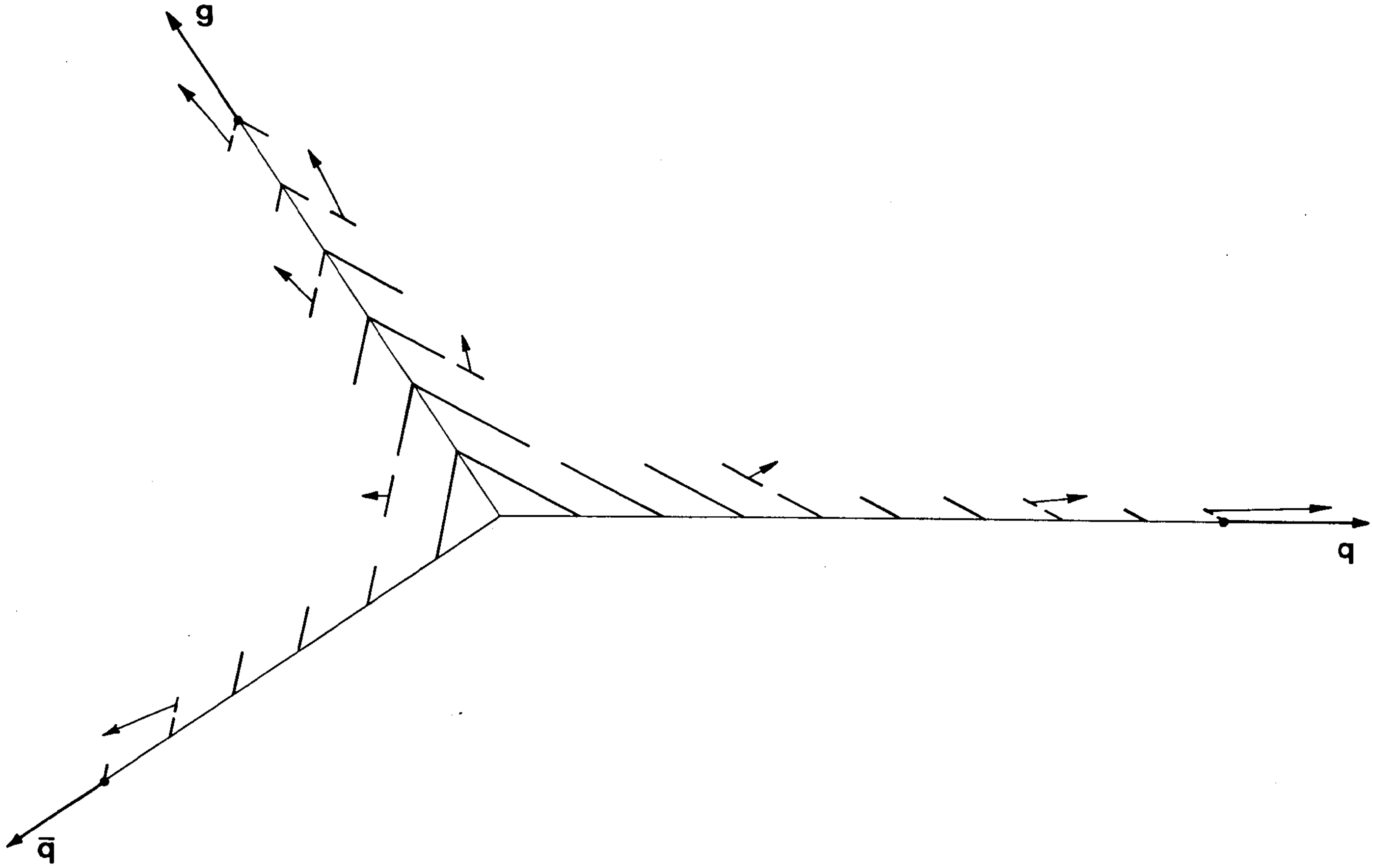

Fig. 2

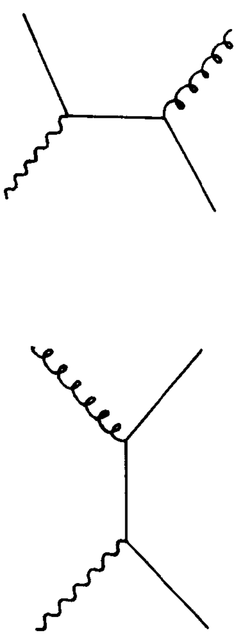

Fig. 1a

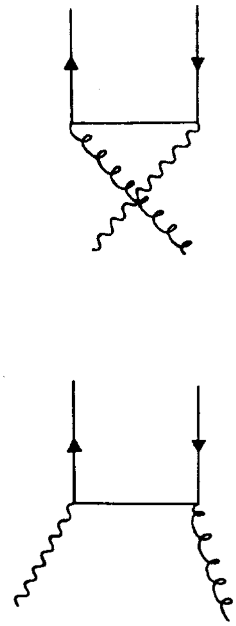

Fig. 1b

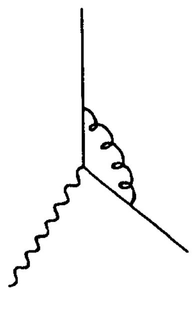

Fig. 1c

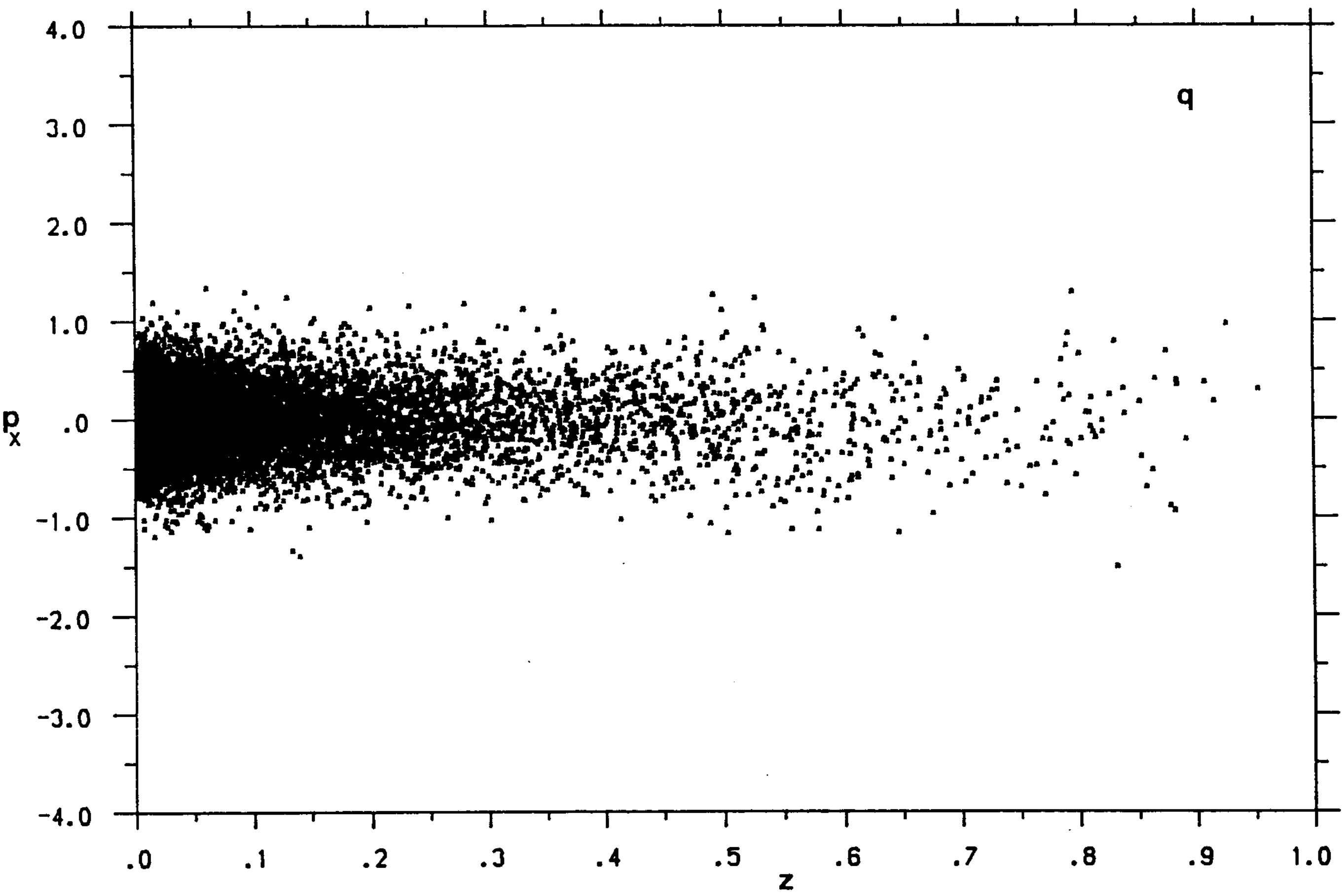

Fig. 4a

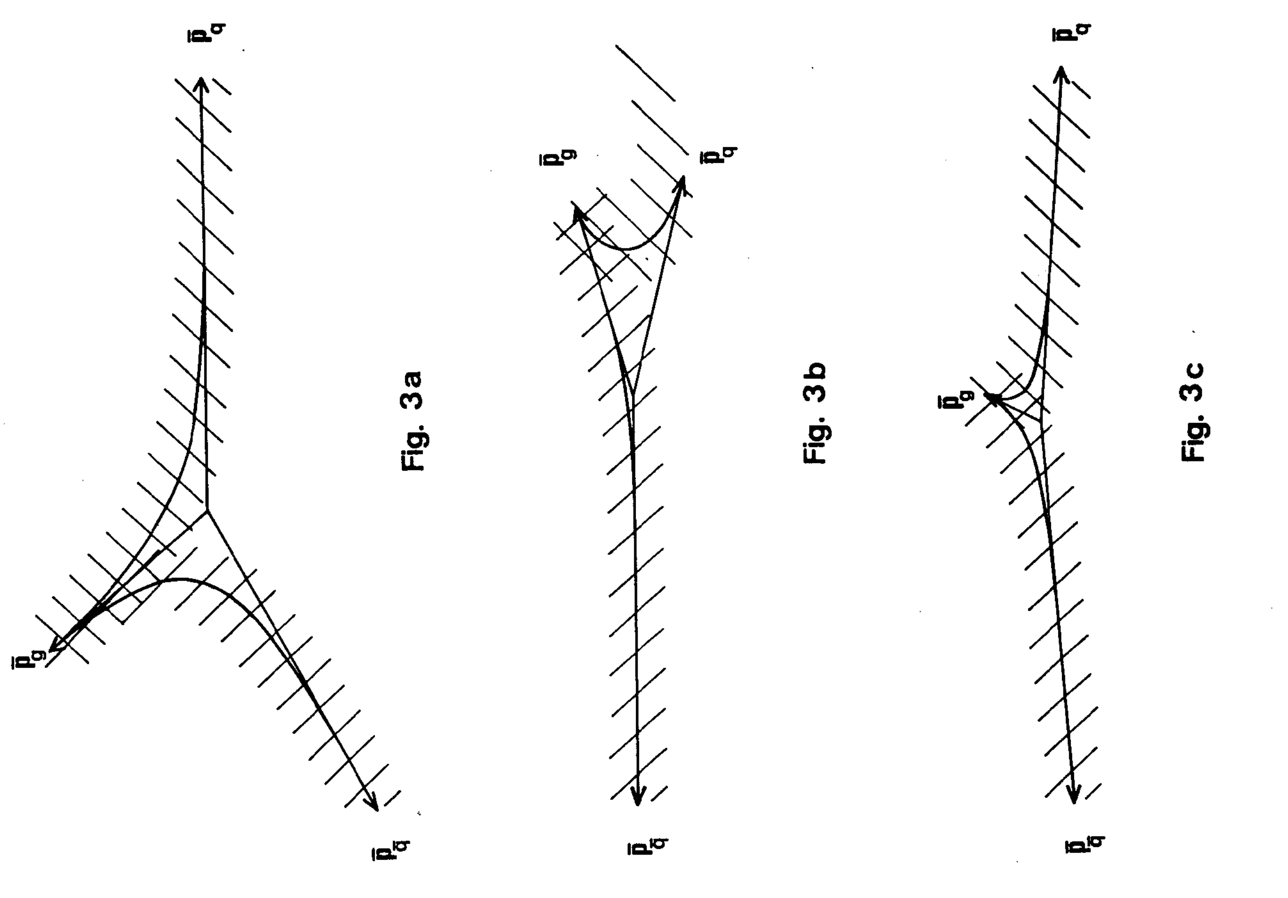

Fig. 3a

Fig. 3b

Fig. 3c

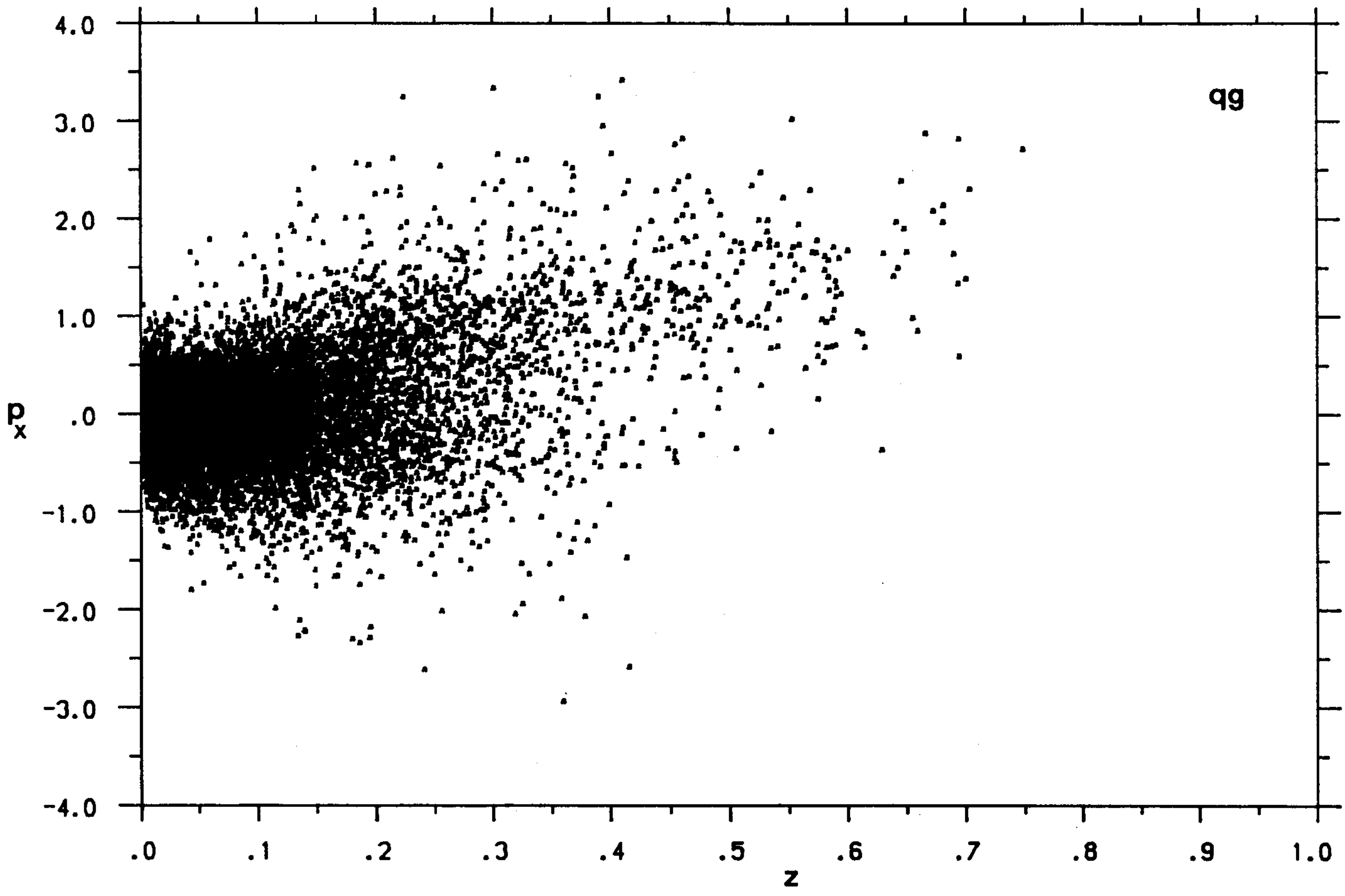
qg
4.0
3.0
2.0
1.0
.0
-1.0
-2.0
-3.0
-4.0
p
x
.0
.1
.2
.3
.4
.5
.6
.7
.8
.9
1.0
z

Fig. 4b

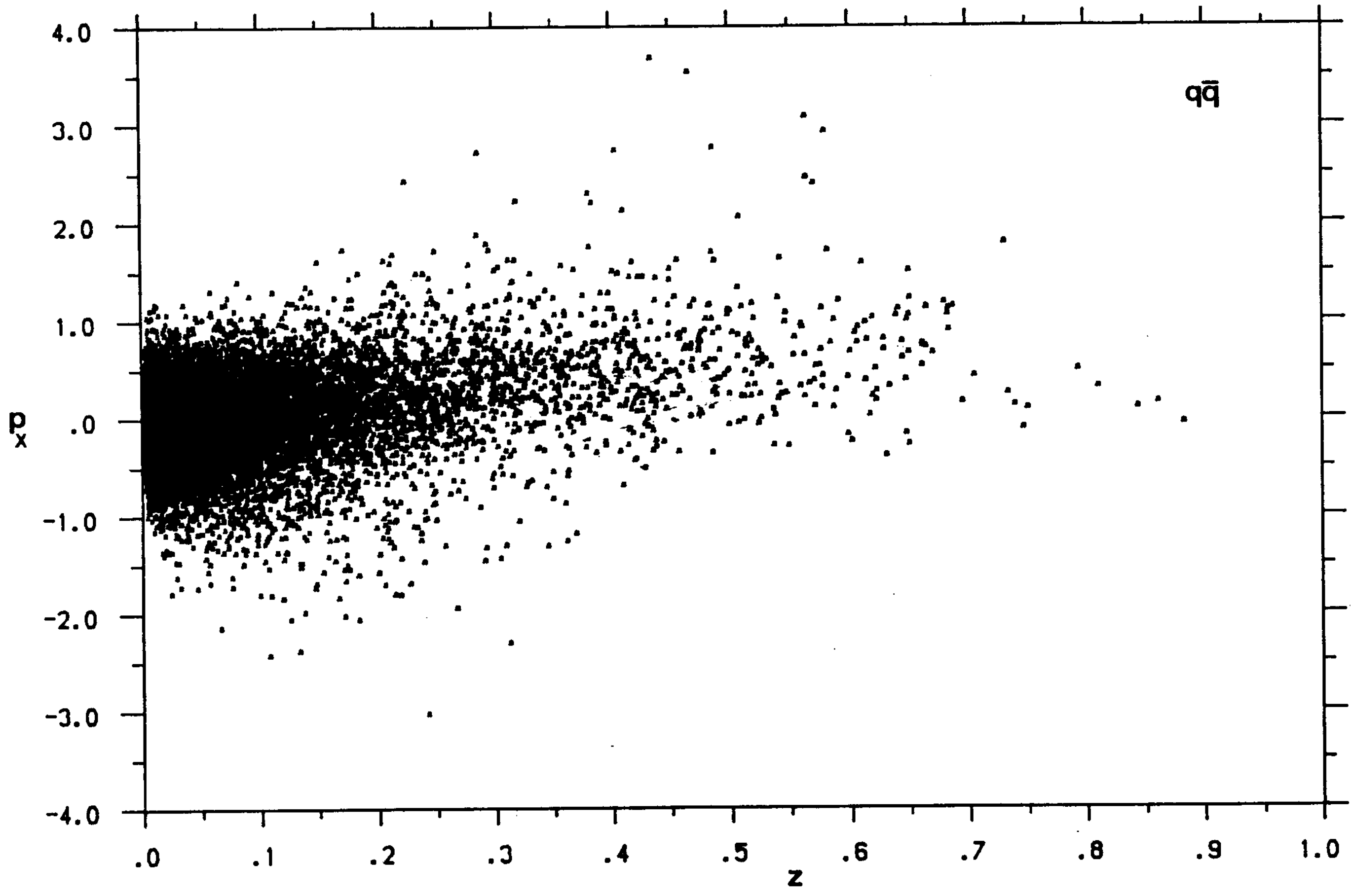
q$\bar{q}$
4.0
3.0
2.0
1.0
.0
-1.0
-2.0
-3.0
-4.0
p
x
.0
.1
.2
.3
.4
.5
.6
.7
.8
.9
1.0
z

Fig. 4c

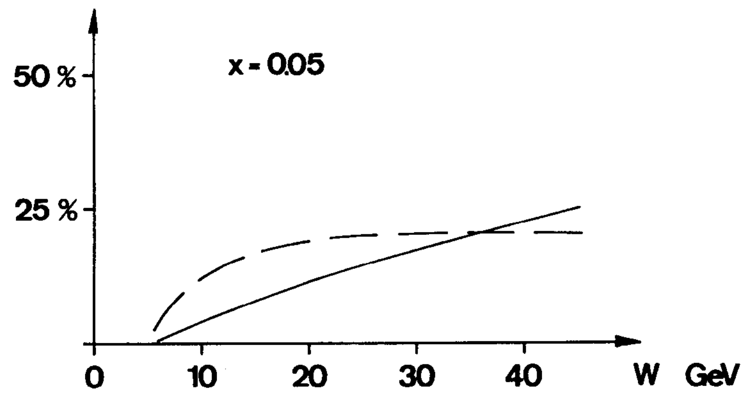

Fig. 4d

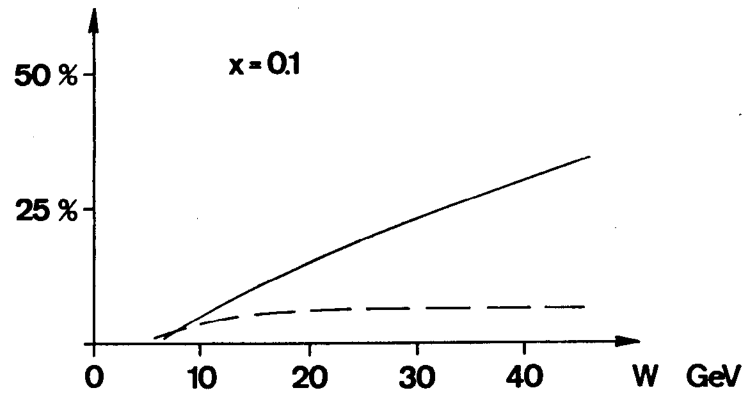

Fig. 4e

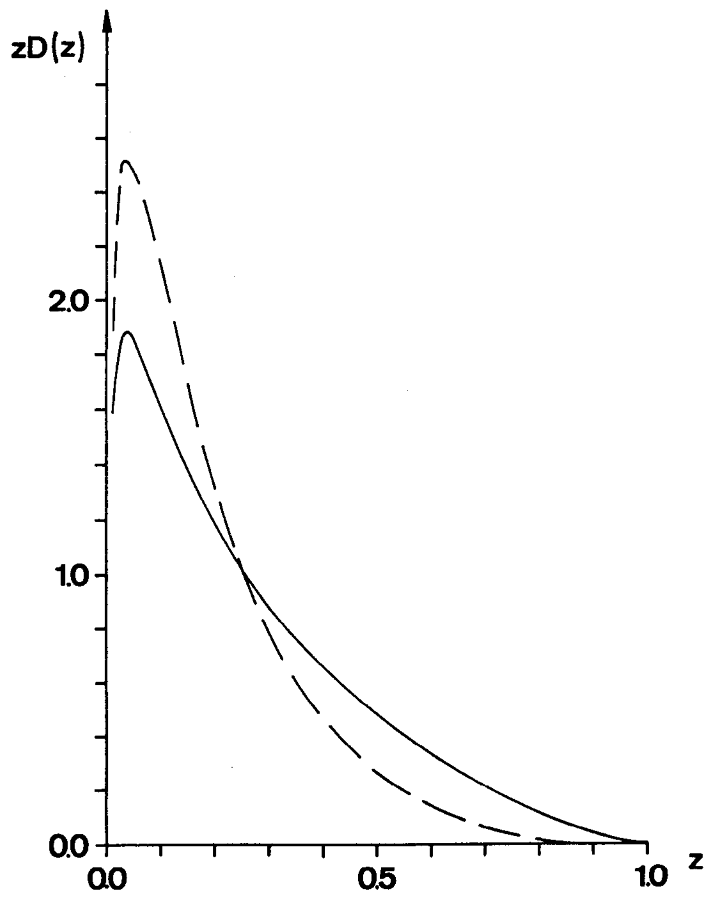

Fig. 5

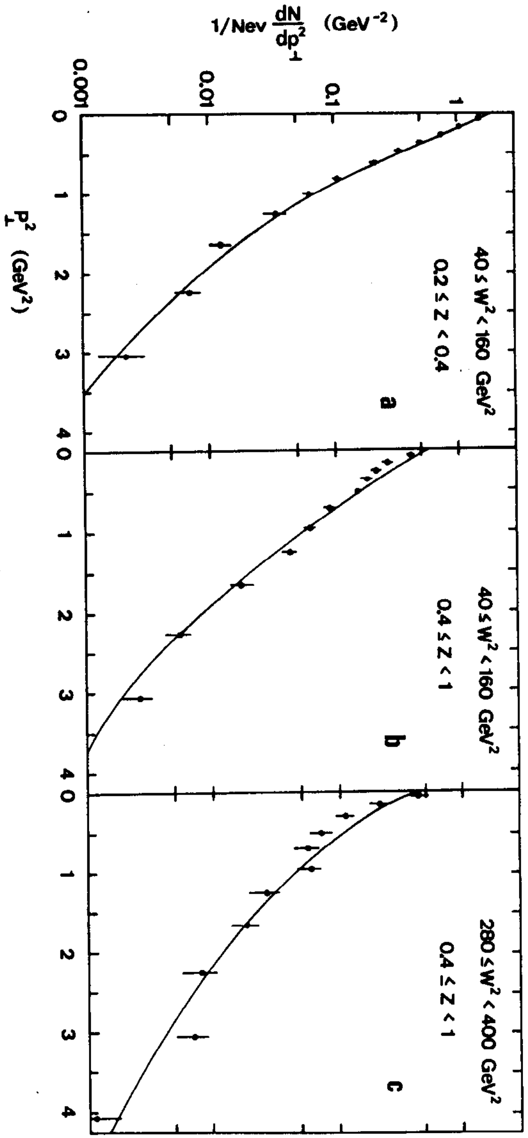
1/Nev dN/dp⊥² (GeV⁻²)
0.001
0.01
0.1
1
0
1
2
3
4
P⊥² (GeV²)
40 ≤ W² < 160 GeV²
0.2 ≤ Z < 0.4
a
40 ≤ W² < 160 GeV²
0.4 ≤ Z < 1
b
280 ≤ W² < 400 GeV²
0.4 ≤ Z < 1
c

Fig. 6

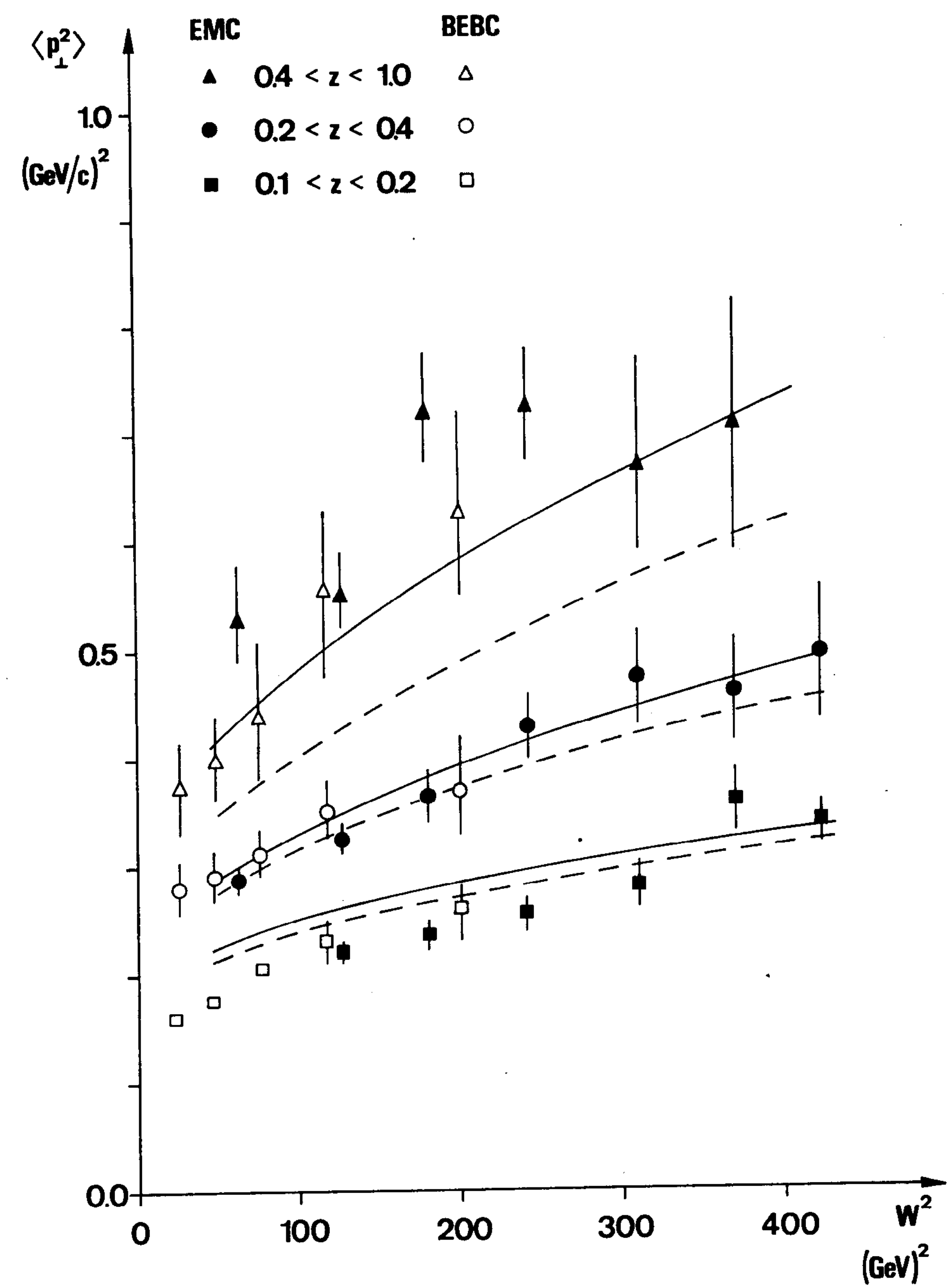
⟨p⊥²⟩
1.0
(GeV/c)²
0.5
0.0
EMC
BEBC
0.4 < z < 1.0
0.2 < z < 0.4
0.1 < z < 0.2
0
100
200
300
400
W²
(GeV)²

Fig. 7

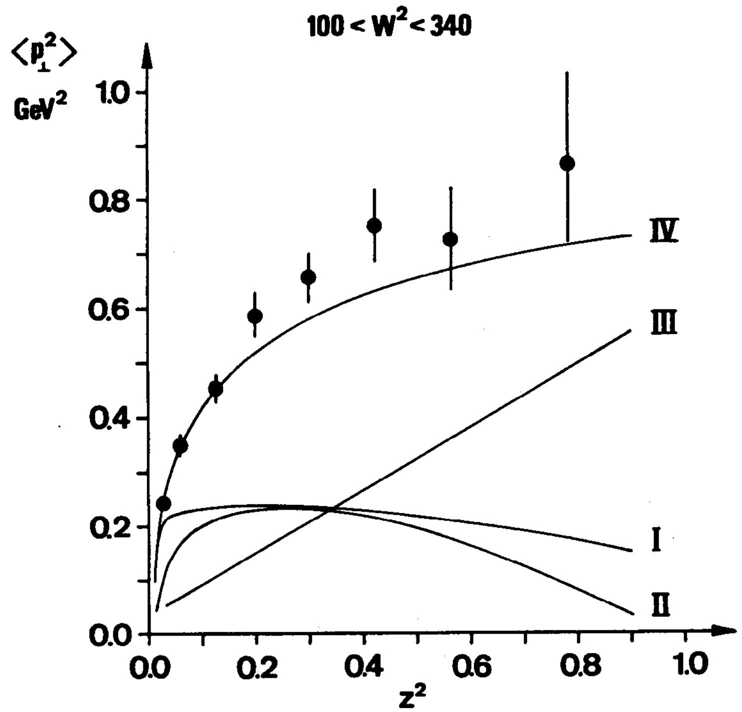
100 < W² < 340
⟨p⊥²⟩
GeV²
1.0
0.8
0.6
0.4
0.2
0.0
0.0
0.2
0.4
0.6
0.8
1.0
z²
IV
III
I
II

Fig. 8

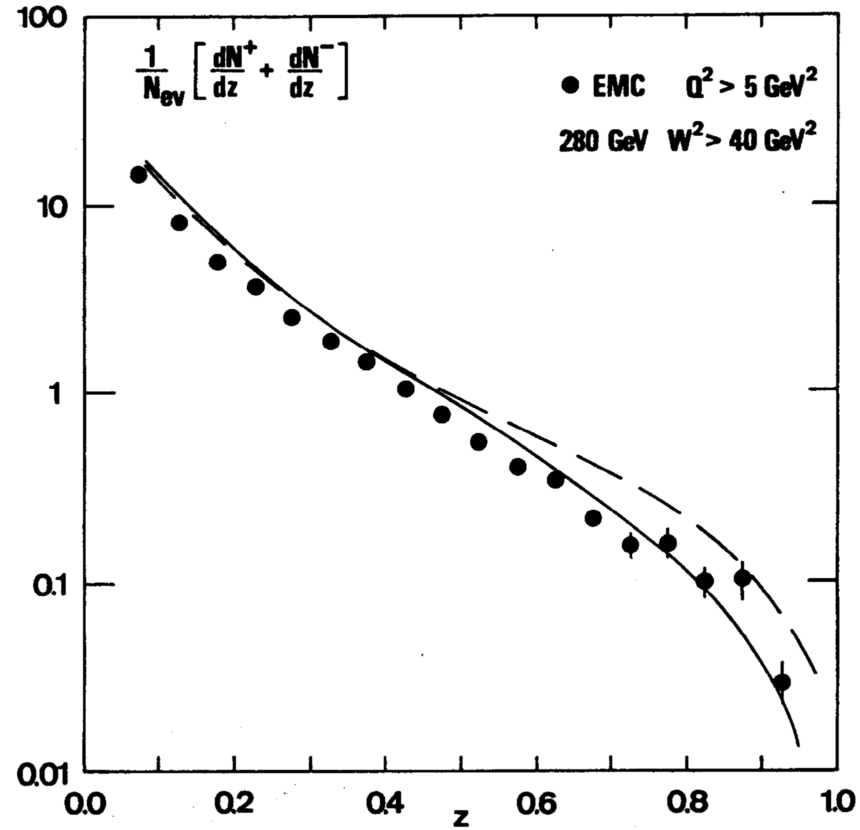
1/N_ev [dN⁺/dz + dN⁻/dz]
● EMC Q² > 5 GeV²
280 GeV W² > 40 GeV²
100
10
1
0.1
0.01
0.0
0.2
0.4
0.6
0.8
1.0
z

Fig. 9

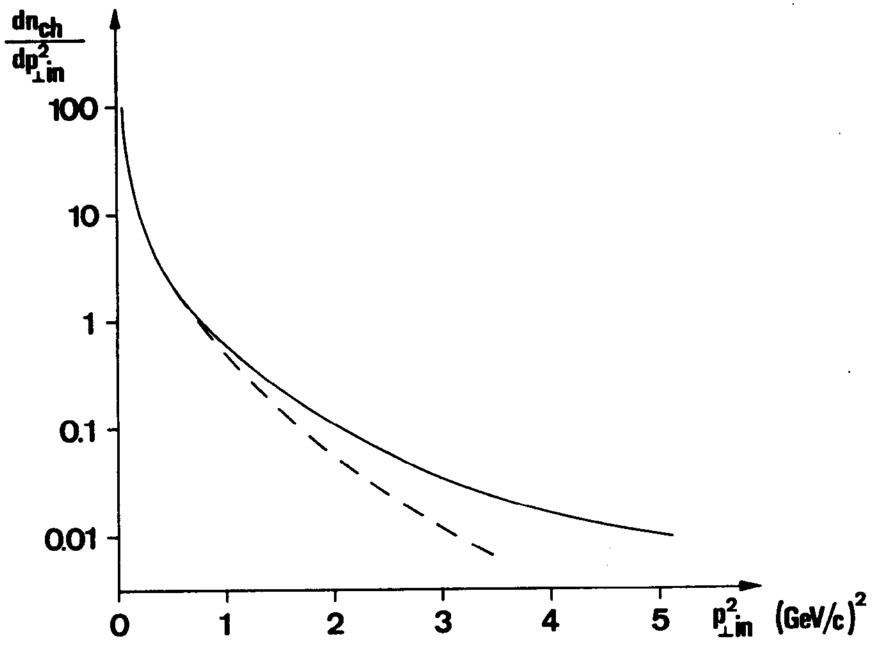

Fig. 10a

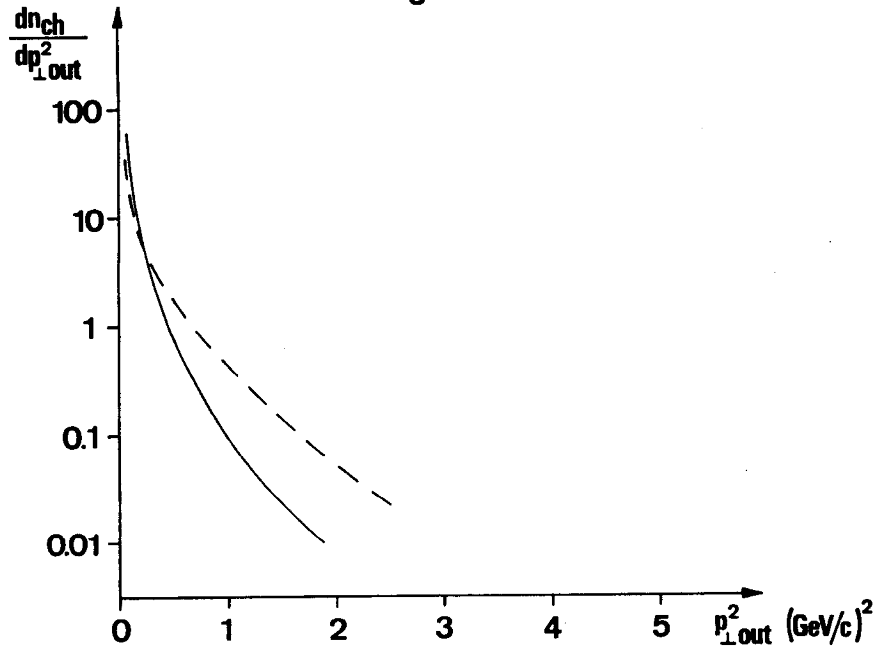

Fig. 10b

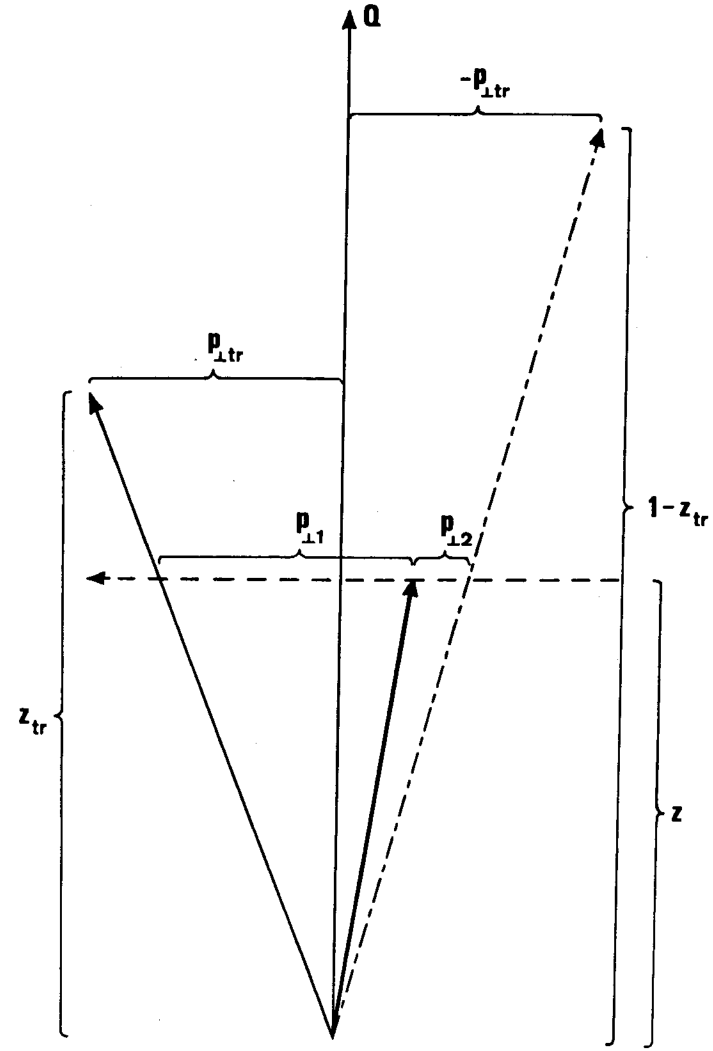

Fig. 11

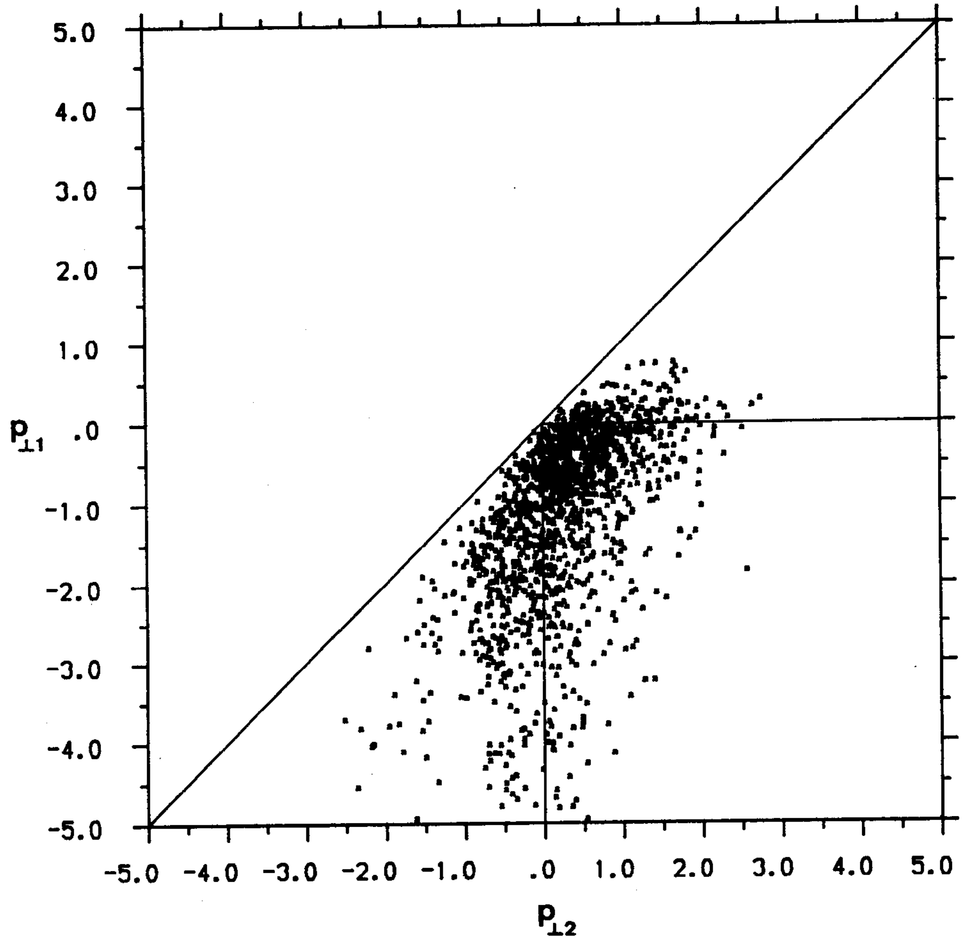

Fig. 12a

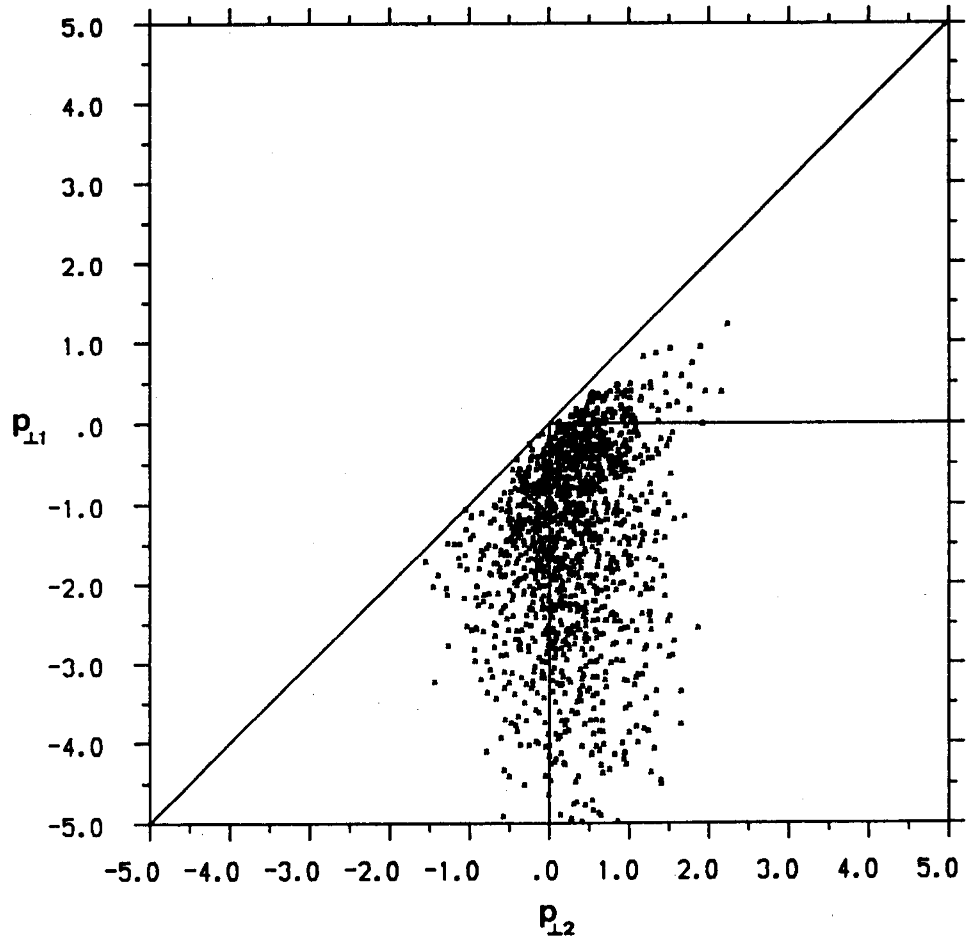

Fig. 12b

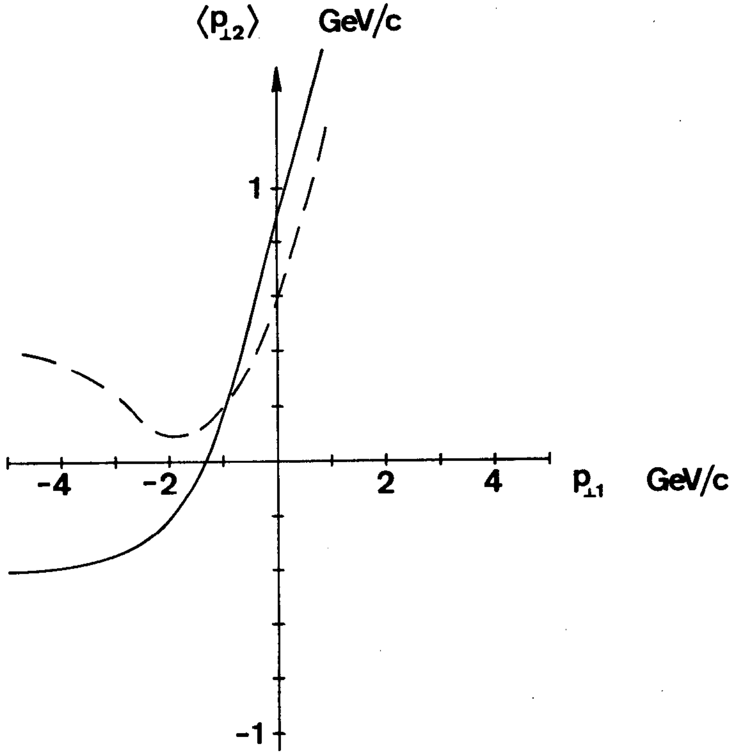

Fig. 12c

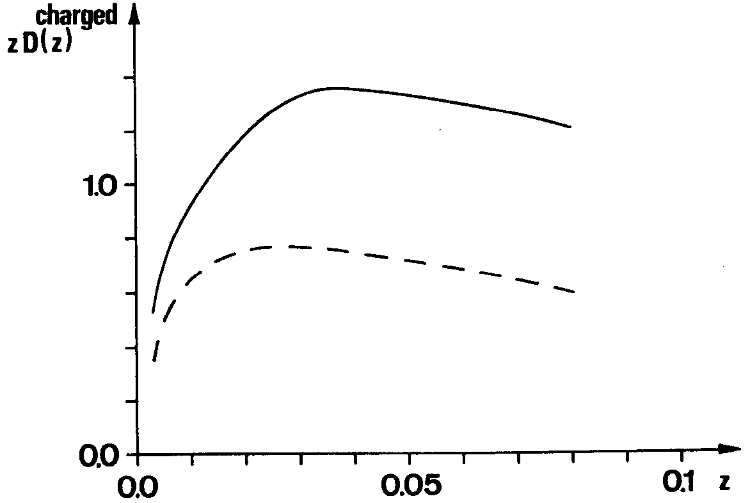

Fig. 13a

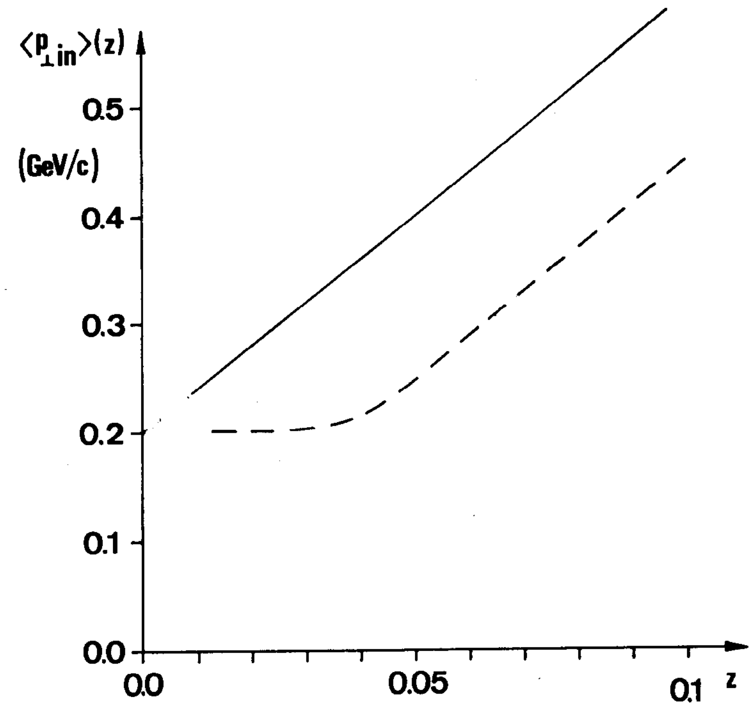

Fig. 13b